# Crossover from Stretched to Compressed Exponential Relaxations in a Polymer-Based Sponge Phase

P. Falus,[1,2] M. A. Borthwick,[2] S. Narayanan,[3] A. R. Sandy,[3] and S. G. J. Mochrie[1]

[1]*Department of Physics, Yale University, New Haven, Connecticut 06511, USA*
[2]*Department of Physics, Massachusetts Institute of Technology, Cambridge, Massachusetts 02139, USA*
[3]*Advanced Photon Source, Argonne National Laboratory, Argonne, Illinois 60439, USA*

X-ray photon correlation spectroscopy was used to characterize the wave vector- and temperature-dependent dynamics of spontaneous thermal fluctuations in a sponge ($L_3$) phase that occurs in a blend of a symmetric poly(styrene-ethylene/butylene-styrene) triblock copolymer with a polystyrene homopolymer. Measurements of the intermediate scattering function reveal a crossover from stretched- to compressed-exponential relaxations as the temperature is lowered from 180 to 120 °C.

Sponge phases are prototypical complex fluids in which amphiphilic molecules in a solvent self-assemble into an extended, random, bilayer membrane that separates space into regions, which may be said to lie either inside (I) or outside (O) the membrane. Tremendous interest has focused on sponge phases in an effort to elucidate their phase stability and mesoscopic structure [1–15]. The difference in I and O volumes ($\psi$) represents an order parameter that is key to theoretical descriptions of the sponge phase [1,2]. In particular, even in the symmetric sponge ($L_3$) phase with unbroken I-O symmetry, the I-O correlation function exhibits a peak at a nonzero wave vector, corresponding to the mean separation between like regions. Although the I-O correlation function itself is inaccessible experimentally, the $L_3$ phase scattering intensity nevertheless exhibits a scattering peak as a result of coupling between $\psi$ fluctuations and the amphiphile density ($\phi$) [15].

Beyond its static properties, several studies have addressed the dynamical behavior of the $L_3$ phase [10,16–26], However, except in a few special cases [21,24], it has so far proven difficult to experimentally examine the relaxation of equilibrium fluctuations at wave vectors ($Q$) most characteristic of the $L_3$ phase, near the peak of the static scattering. On the theoretical side, Milner *et al.* [16] have given a physically appealing formulation that postulates three slow modes: one associated with $\phi$, another associated with $\psi$, and the third corresponding to topological relaxation, via the creation and dissolution of membrane necks. The latter processes are activated. Therefore, topological relaxation may be expected to be especially slow. Alternatively, Gompper and Hennes [19,20] have presented field-theoretic calculations that incorporate the coupling between $\psi$ and $\phi$ required to explain the observed $L_3$-phase static scattering. They also incorporate couplings of $\psi$ and of $\phi$ to the transverse momentum density, which they include as an additional slow variable.

Here we report multispeckle x-ray photon correlation spectroscopy (XPCS) measurements [27–31] of the $L_3$ phase that occurs in blends of a poly(styrene-ethylene/butylene-styrene) triblock copolymer (PSEBS) with a polystyrene homopolymer (PS) [32]. Remarkably, these data show a crossover from stretched- to compressed-exponential relaxation as the temperature is decreased from 180 to 120 °C, even though the static structure evolves only slightly within this temperature range. [Note that 120 °C lies well above the bulk PS glass transition temperature ($T_g$) [33], although the actual $T_g$ of the PS component here may be lower than the bulk value because of its nanoconfinement within an $L_3$ phase [34].] As far as we are aware, such behavior has not previously been observed in any system and suggests that the $L_3$ phase may undergo a thermally driven jamming transition [35] from a fluid state at higher temperatures to a jammed state at lower temperatures.

Blends of 0.20 volume fraction PSEBS ($M_w = $ 83.6 kg/mole, $M_w/M_n = 1.07$) and 0.80 volume fraction PS ($M_w = 4.82$ kg/mole, $M_w/M_n = 1.11$) were prepared as described previously [32] and then annealed under vacuum at 160 °C for several days, prior to x-ray measurements at beam line 8-ID at the Advanced Photon Source (APS). The samples' small-angle-x-ray-scattering profiles (Fig. 1) show the peak at zero $Q$ and the peak at nonzero $Q$ that together are characteristic of an $L_3$ phase [4,9,15]. The solid lines in the figure are best fits using the $L_3$-phase line shape of Refs. [15,32].

XPCS measures the intensity autocorrelation function [$g_2(Q, t)$] defined as

$$g_2(Q, t) = \frac{\langle I(Q, t')I(Q, t' + t)\rangle}{\langle I(Q, t')\rangle^2}, \qquad (1)$$

where $I(Q, t')$ is the scattered intensity at wave vector $Q$ and time $t'$. $t$ is the delay time, and the brackets $\langle \cdots \rangle$ signify an ensemble average over different speckles and over $t'$. $g_2(Q, t)$ is related to the normalized intermediate scattering function (ISF) [$f(Q, t)$] via $g_2(Q, t) = 1 + A[f(Q, t)]^2$, where $A$ is the speckle contrast. Experimental $g_2$s were acquired as described in Ref. [30] and then fitted using both a stretched/compressed-exponential form for
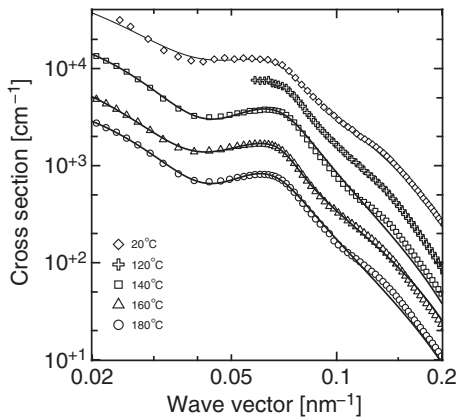
FIG. 1.  $I(Q)$ vs $Q$ for the PSEBS-PS $L_3$ phase at 20 (diamonds), 120 (crosses), 140 (squares), 160 (triangles), and 180 °C (circles), plotted on a log-log scale. For clarity, data for the different temperatures have been muliplied by factors of 16, 8, 4, 2, and 1, respectively. For 120 °C, we show only $I(Q)$ obtained from the time-resolved data of this Letter.

the ISF, $f(Q, t) = \exp[-(\Gamma t)^\beta]$, with $\Gamma$ and $\beta$ as fitting parameters, and a double-exponential form for the ISF, $f(Q, t) = a_F \exp(-\Gamma_F t) + a_S \exp(-\Gamma_S t)$, with $a_S = 1 - a_F$, $\Gamma_F$, and $\Gamma_S$ ($\Gamma_F > \Gamma_S$) as fitting parameters. Both forms yield a good description of the data. For technical reasons, the longest time delay accessible was 170 s [30], preventing determination of the ISF for $Q < 0.058$ nm$^{-1}$ at 120 °C and for $Q < 0.017$ nm$^{-1}$ at 140 °C.

A selection of the corresponding normalized ISFs, obtained at 180 °C, are plotted in Fig. 2 on a logarithmic scale versus reduced delay time ($\Gamma_I t$) on a linear scale, where $\Gamma_I = a_F \Gamma_F + a_S \Gamma_S$ is the initial decay rate, determined from the double-exponential fits. The logarithmic intensity and linear time scale of this figure imply that simple exponentials would appear as straight lines. Evidently, the measured ISFs at 180 °C exhibit a positive curvature, indicating stretched-exponential or double-exponential behavior of the ISF. The solid lines in this figure correspond to the best fits to the double-exponential form, corresponding to two coupled slow variables [36].

In striking contrast to the data at 180 °C, at 120 °C the ISFs, plotted on logarithmic intensity and linear time axes in Fig. 3, show negative curvature. Thus, at 120 °C, the ISF exhibits a *compressed-exponential* form (solid lines). It is also possible to achieve good fits to these data using a double exponential, but with a *negative* weight for the fast decay mode. Such an ISF requires a reactive coupling between slow variables [36]. Although the couplings, introduced in Ref. [19], between both $\psi$ and $\phi$ and the transverse momentum density are indeed reactive (and nonlinear), it is unlikely that these would become dominant as the PS viscosity is increased [19]. Instead, we seek an alternative explanation of the dramatic change in behavior observed.

Recently, it has been proposed [35] that a wide range of highly structured but disordered soft matter—including
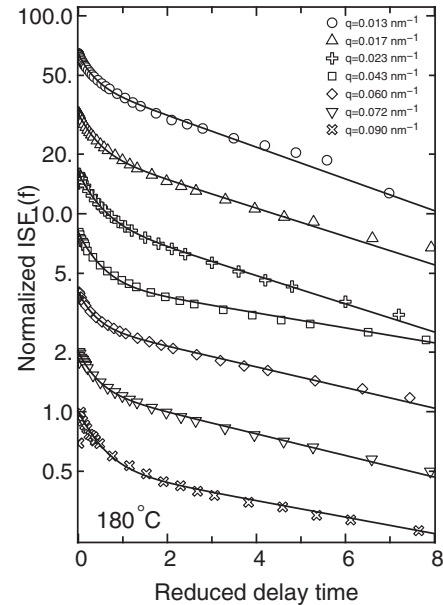


FIG. 2.  ISFs ($f$) vs reduced delay time ($\Gamma_I t$) for several wave vectors at 180 °C. For clarity, successive ISFs have been multiplied by factors of 1, 2, 4, 8, 16, 32, and 64, respectively. Solid lines are best fits to a double-exponential form for the ISF.

gels [37], foams [38], clays [29], suspensions [39–41], and emulsions [42]—can exhibit a *jamming* transition from a fluid to a solidlike state with arrested dynamics. Moreover, a variety of materials in a putative jammed state display compressed-exponential ISFs [29,37,42], suggesting that such ISFs may be a key signature of the jammed state. Such a form for the ISF has been explained on the
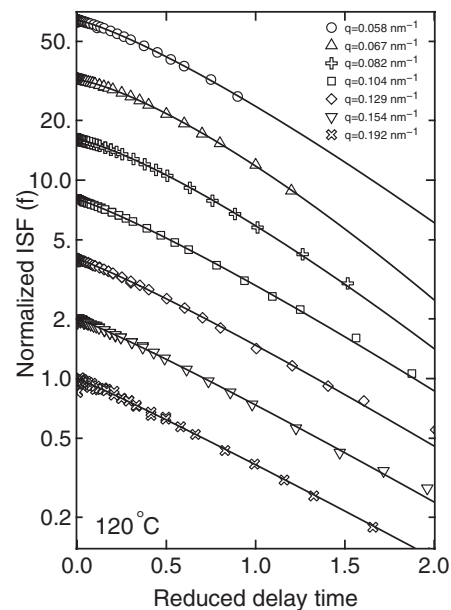


FIG. 3.  ISFs ($f$) vs reduced delay time ($\Gamma t$) for several wave vectors at 120 °C. For clarity, successive ISFs have been multiplied by factors of 1, 2, 4, 8, 16, 32, and 64, respectively. Solid lines are the best fits to a stretched/compressed form for the ISF.

PRL **97**, 066102 (2006)

P H Y S I C A L   R E V I E W   L E T T E R S

week ending
11 AUGUST 2006

basis of the relaxation of force dipoles randomly distributed throughout the sample [37,42,43]. This picture also predicts a linear variation of the characteristic relaxation rate with $Q$. The jammed state often undergoes aging, which is manifested as an decrease in the characteristic relaxation rate with aging time [29,37,41,42]. In the present case, data obtained at $120\,°C$ after an aging time of $7000\,s$ are indistinguishable from those obtained after an aging time of $15\,000\,s$ (data not shown). It follows that any aging-time dependence of the relaxation rate at $120\,°C$ within this time range would have to be much weaker than those reported in Refs. [29,37,41]. However, aging-time-independent behavior has also been reported in Ref. [42].

We summarize in Fig. 4 our results for the $Q$ dependence of the *reduced* relaxation rates, defined as $\Gamma_R = \Gamma_M/\Gamma_0$, where $\Gamma_M$ is one of $\Gamma_F$, $\Gamma_S$, or $\Gamma$, and $\Gamma_0 = k_B T Q^2 Q_0/\eta_{PS}$, with $Q_0$ the peak of the I-O correlation function ($0.036\,nm^{-1}$) and $\eta_{PS}$ the temperature-dependent viscosity of the PS solvent [33], which varies from $7\,P$ at $180\,°C$ to $2200\,P$ at $120\,°C$. Also shown in this figure is the reduced relaxation rate for PSEBS-in-PS vesicles from Ref. [32]. In that case, data from 140, 160, and $180\,°C$ collapse quite well to the theoretical curve (solid line) for isolated membrane plaquettes, for which the relaxation rate shows a $Q^3$ variation [44]. By contrast, for the present data
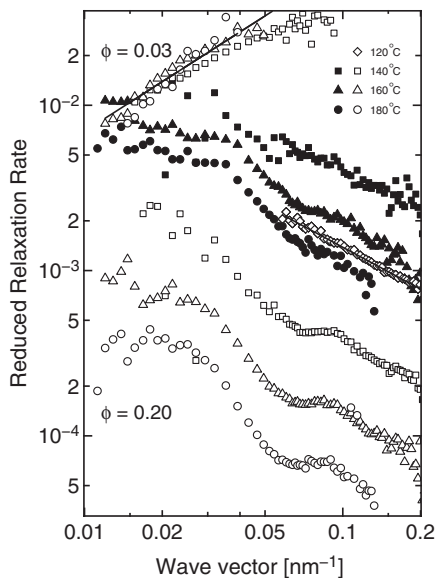


FIG. 4. Reduced relaxation rate vs $Q$. At $120\,°C$, the open diamonds correspond to the $\Gamma$s from stretched-exponential fits. At 140, 160, and $180\,°C$, respectively, the solid squares, triangles, and circles correspond to the fast mode ($\Gamma_F$), while the open squares, triangles, and circles correspond to the slow mode ($\Gamma_S$), as determined from double-exponential fits. The solid line through the $120\,°C$ data corresponds to a $Q^{1.16}$ variation of the relaxation rate. Also shown are the relaxation rates from Ref. [32] obtained at 140, 160, and $180\,°C$ for a PSEBS volume fraction of $\phi = 0.03$. The line through these data corresponds to the theoretical prediction of Ref. [44].

at 140, 160, and $180\,°C$, although in both cases the $Q$ dependence appears similar at the different temperatures, neither $\Gamma_F/\Gamma_0$ (solid symbols) nor $\Gamma_S/\Gamma_0$ collapse to a single curve: $\Gamma_F/\Gamma_0$ increases by a factor of 1.5–2 as the temperature is decreased from 180 to $160\,°C$ and again from 160 to $140\,°C$, while $\Gamma_S/\Gamma_F$ increases by factors of about 3 for the same temperature steps. These observations suggest that, in addition to solvent flow, processes, such as solvent permeation through the membrane, that do not depend on the solvent viscosity are relevant for both modes. Both $\Gamma_F/\Gamma_0$ and $\Gamma_S/\Gamma_0$ appear independent of $Q$ for $Q \leq 0.03\,nm^{-1}$, indicating diffusive behavior on long length scales. A notable feature of both $\Gamma_F/\Gamma_0$ and $\Gamma_S/\Gamma_0$ is a minimum, more pronounced for $\Gamma_S/\Gamma_0$, occurring at or close to the value of $Q$, at which there is a peak in the static scattering (Fig. 1). This is the well-known phenomenon of "de Gennes narrowing" [45]. Surprisingly, at larger $Q$s, the relaxation rates do not show the $Q^3$ dependence expected for independent membranes [21,24–26] and found at smaller $Q$s in the more dilute system [32]. Turning now to the data obtained at $120\,°C$, no minimum in $\Gamma/\Gamma_0$ is discernible. Instead, over the range of $Q$s studied, which includes the peak of the static scattering, there is a smooth variation of the relaxation rate with $Q$, which may be described as a power law with an exponent of $1.16 \pm 0.05$ (solid line in the figure), similar to, but slightly larger than, the linear variation observed previously in the case of compressed-exponential relaxations [37,41,42].

The relative amplitude of the slow mode ($a_S$) for the double-exponential fits at 140, 160, and $180\,°C$ is shown versus $Q$ in Fig. 5(a). Overall, the amplitude of the slow decay increases towards unity with decreasing temperature, with the effect that the ISFs appear progressively less stretched as the temperature decreases. In addition, at each temperature, $a_S$ shows a peak occurring at the $Q$ of the peak of the static scattering, which we interpret as a further manifestation of de Gennes narrowing. Figure 5(b) shows the best-fit exponent ($\beta$) versus $Q$, determined from the
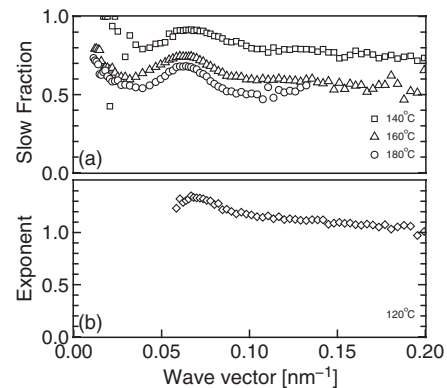


FIG. 5. (a) Best-fit relative amplitude of the slow relaxation ($a_S$) vs $Q$ from fits using a double-exponential form for the ISF at 140 (squares), 160 (triangles), and $180\,°C$ (circles). (b) Best-fit stretching/compression exponent from fits using a stretched/compressed-exponential form for the ISF.

066102-3

compressed-exponential fits at 120 °C. Evidently, the exponent varies from a peak of about 1.35 at 0.07 nm$^{-1}$—the peak of the static scattering again—to 1.07 at the largest $Q$s studied (0.2 nm$^{-1}$). This behavior differs from that of Ref. [29], which probed $Q$s corresponding to the scattering peak in an aging Laponite suspension. There the compression exponent ($\simeq$1.5) was independent of $Q$. Nevertheless, the compressed-exponential relaxation found for the PSEBS-in-PS $L_3$ phase at 120 °C [Figs. 3 and 5(b)], together with a relaxation rate that varies approximately linearly with $Q$, supports the idea that the PSEBS-in-PS $L_3$ phase becomes jammed on cooling to 120 °C.

How could jamming occur in this case? Beyond Ref. [16], several experiments indicate that topological relaxations can be very slow in the $L_3$ phase [18,23,46] and in the analogous bicontinuous microemulsion phase [47]. Therefore, we propose that the origin of jamming in the present case involves the arrest of topological relaxation. Specifically, we hypothesize that, although the static structure is similar at the different temperatures studied, nevertheless, changing the temperature causes the equilibrium topology to vary, for example, by changing slightly the equilibrium mean separation between membranes and the equilibrium thickness of the membrane. We further hypothesize that, for 140 °C and above, the membrane topology is able to equilibrate, but that, because topological equilibration is activated and hence increasingly slow at lower temperatures and because collective diffusion is itself slowed because of the increased PS viscosity, at 120 °C, the membrane topology does not equilibrate within the duration of the experiment. Under this constraint, the sponge structure will be subject to internal stresses associated with its topological frustration. Specifically, there will be a free energy cost per unit area associated with the deficit/surplus of membrane necks; i.e. the membrane will acquire a surface tension. According to this interpretation, the deformations that occur as a result of these internal stresses are then the origin of the relaxation of the ISF observed at 120 °C, following Refs. [29,37,42]. Also according to this interpretation, at 140, 160, and 180 °C, the present data represent the first determination of the equilibrium dynamics of a polymer $L_3$ phase. These data are well described in terms of two modes, with a strongly temperature-dependent relative amplitude. In addition, both modes are diffusive at small $Q$ and, near the peak of the static scattering, manifest de Gennes narrowing in both their rates and their relative amplitude. In principle, the theories of Refs. [19,20] should be able to explain these results.

[1] M. E. Cates *et al.*, Europhys. Lett. **5**, 733 (1988).
[2] D. A. Huse and S. Leibler, J. Phys. (Paris) **49**, 605 (1988).
[3] D. Anderson, H. Wennerstrom, and U. Olsson, J. Phys. Chem. **93**, 4243 (1989).
[4] G. Porte *et al.*, J. Phys. (Paris) **50**, 1335 (1989).
[5] L. Golubovic and T. C. Lubensky, Phys. Rev. A **41**, 4343 (1990).
[6] G. Gompper and M. Schick, Phys. Rev. B **41**, 9148 (1990).
[7] D. Roux *et al.*, Europhys. Lett. **9**, 229 (1990).
[8] C. Coulon, D. Roux, and A. M. Bellocq, Phys. Rev. Lett. **66**, 1709 (1991).
[9] M. Skouri *et al.*, J. Phys. II (France) **1**, 1121 (1991).
[10] G. Porte *et al.*, J. Phys. II (France) **1**, 1101 (1991).
[11] D. Roux, C. Coulon, and M. E. Cates, J. Phys. Chem. **96**, 4174 (1992).
[12] H. Wennerstrom and U. Olsson, Langmuir **9**, 365 (1993).
[13] D. C. Morse, Phys. Rev. E **50**, R2423 (1994).
[14] L. Golubovic, Phys. Rev. E **50**, R2419 (1994).
[15] G. Gompper and M. Schick, Phys. Rev. E **49**, 1478 (1994).
[16] S. T. Milner, M. E. Cates, and D. Roux, J. Phys. (Paris) **51**, 2629 (1990).
[17] R. Granek and M. E. Cates, Phys. Rev. A **46**, 3319 (1992).
[18] G. Waton and G. Porte, J. Phys. II (France) **3**, 515 (1993).
[19] G. Gompper and M. Hennes, J. Phys. II (France) **4**, 1375 (1994).
[20] M. Hennes and G. Gompper, Phys. Rev. E **54**, 3811 (1996).
[21] E. Freyssingeas, F. Nallet, and D. Roux, Langmuir **12**, 6028 (1996).
[22] M. Nonomura and T. Ohta, J. Chem. Phys. **110**, 7516 (1999).
[23] B. Schwarz *et al.*, Langmuir **16**, 8643 (2000).
[24] M. Mihailescu *et al.*, J. Chem. Phys. **115**, 9563 (2001).
[25] S. Komura *et al.*, Phys. Rev. E **63**, 041402 (2001).
[26] O. Holderer *et al.*, J. Chem. Phys. **122**, 094908 (2005).
[27] S. B. Dierker *et al.*, Phys. Rev. Lett. **75**, 449 (1995).
[28] S. G. J. Mochrie *et al.*, Phys. Rev. Lett. **78**, 1275 (1997).
[29] R. Bandyopadhyay *et al.*, Phys. Rev. Lett. **93**, 228302 (2004).
[30] P. Falus, M. A. Borthwick, and S. G. J. Mochrie, Rev. Sci. Instrum. **75**, 4383 (2004).
[31] P. Falus, M. A. Borthwick, and S. G. J. Mochrie, Phys. Rev. Lett. **94**, 016105 (2005).
[32] P. Falus *et al.*, Phys. Rev. Lett. **93**, 145701 (2004).
[33] T. G. Fox and P. J. Flory, J. Appl. Phys. **21**, 581 (1950).
[34] C. J. Ellison and J. M. Torkelson, Nat. Mater. **2**, 695 (2003).
[35] A. J. Liu and S. R. Nagel, Nature (London) **396**, 21 (1998).
[36] D. Forster, *Hydrodynamic Fluctuations, Broken Symmetry, and Correlation Functions* (Benjamin, Reading, MA, 1975).
[37] L. Cipelletti *et al.*, Phys. Rev. Lett. **84**, 2275 (2000).
[38] C. S. O'Hern *et al.*, Phys. Rev. Lett. **86**, 111 (2001).
[39] V. Trappe *et al.*, Nature (London) **411**, 772 (2001).
[40] P. N. Pham *et al.*, Science **296**, 104 (2002).
[41] M. Bellour *et al.*, Phys. Rev. E **67**, 031405 (2003).
[42] L. Cipelletti *et al.*, Faraday Discuss. **123**, 237 (2003).
[43] J.-P. Bouchard and E. Pitard, Eur. Phys. J. E **6**, 231 (2001).
[44] A. G. Zilman and R. Granek, Phys. Rev. Lett. **77**, 4788 (1996).
[45] P. G. de Gennes, Physica (Amsterdam) **25**, 825 (1956).
[46] L. Porcar *et al.*, Phys. Rev. Lett. **93**, 198301 (2004).
[47] U. Peter, D. Roux, and A. K. Sood, Phys. Rev. Lett. **86**, 3340 (2001).